

Phase diagram of a mesoscopic superconducting Pb square: Ballistic Hall magnetometry

K. Vervaeke,^{1,2} K. De Keyser,¹ M. Menghini,¹ C. Carballeira,³ G. Borghs,² and V. V. Moshchalkov¹
¹INPAC-Institute for Nanoscale Physics and Chemistry, K.U.Leuven, Celestijnenlaan 200D, Leuven B-3001, Belgium
²Interuniversity Microelectronics Center (IMEC vzw), Kapeldreef 75, Leuven B-3001, Belgium
³LBTS, Departamento de Física da Materia Condensada, Universidade de Santiago de Compostela, Santiago de Compostela E-15782, Spain

(Received 13 August 2007; published 7 November 2007)

Ballistic Hall magnetometry is used to investigate the magnetization of a mesoscopic superconducting Pb square as a function of magnetic field (H) and temperature (T). Vortex penetration and expulsion fields are determined from magnetization curves at different temperatures below T_c and are combined in an experimental T - H phase diagram. Enhanced stability of the symmetry-matching vorticities $L=1$ and $L=4$ is observed. The experimental results are compared with theoretical calculations using the nonlinear Ginzburg-Landau theory for a thin square.

DOI: [10.1103/PhysRevB.76.184506](https://doi.org/10.1103/PhysRevB.76.184506)

PACS number(s): 74.78.Na, 74.25.Ha, 74.25.Dw

I. INTRODUCTION

The study of mesoscopic type II superconductors has attracted the attention of many theoretical and experimental groups during the past 10 yr. In these systems, the confinement of the superconducting condensate gives rise to exotic phase transitions and vortex configurations that differ from the Abrikosov lattice, which is the lowest energy state in macroscopic ideal samples.

The superconducting phase boundary $T_c(H)$ of mesoscopic regular polygons has been determined using transport measurements.¹⁻³ From the theoretical point of view, the $T_c(H)$ curve of such samples has been obtained using the linearized Ginzburg-Landau (GL) equations.¹⁻³ These calculations show that in mesoscopic regular polygons, the formation of vortex-antivortex pairs is favored when the number of vortices is not compatible with the discrete symmetry of the sample. Good agreement with the critical temperature vs magnetic field curve $T_c(H)$ obtained experimentally in Al samples is observed, supporting the idea of the spontaneous formation of antivortices in small superconducting polygons at the phase boundary.^{1,2} Experimental evidence for the formation of giant vortex states⁴ in small samples has been presented in Refs. 5 and 6. Very recently, the Bitter decoration technique has allowed the observation of vortex configuration in mesoscopic circular, square, and triangular Nb samples deeper in the superconducting state.⁷ In the case of disks, it is observed that vortices arrange themselves by forming concentric shells as the magnetic field is increased. Thanks to the advance in the fabrication of nanoscale Hall probes, it was possible to study the magnetization of individual small samples.^{8,9} Jumps in the magnetization are observed as the field increases (decreases) corresponding to the penetration (expulsion) of flux quanta in the sample. One characteristic feature of the magnetization of individual mesoscopic samples is the hysteresis observed between flux penetration and expulsion curves. This behavior is associated with the Bean-Livingston surface barrier¹⁰ that affects the entry and the exit of vortices. The effects of this barrier have been studied using the time-dependent Ginzburg-Landau equations.¹¹ This analysis confirms that metastability appears

due to the presence of the surface barrier, leading to hysteresis in the magnetic response.

The transition lines between states with different vorticities L , which is the number of flux quanta inside the sample, deep inside the superconducting phase can be obtained by measuring magnetization loops.⁹ Stability of particular vortex patterns imposed by the sample geometry has been reported. Using the full nonlinear GL [functional Ginzburg-Landau (FGL)] equations, Chibotaru *et al.*^{3,12} and Carballeira *et al.*¹³ have studied the stability of the vortex patterns formed in mesoscopic square and triangle in a broad range of magnetic fields and temperatures. Experimentally, these vortex patterns have not been studied yet.

In this paper, we present the Hall magnetometry experiments in a micro-sized Pb square, aimed at the experimental verification of the theoretical prediction of a variety of vortex phases in superconducting microsquares. We determine the transition lines between vortex states with different L . We also compare, both qualitatively and quantitatively, the experimental results with theoretical calculations based on the FGL equations.

II. EXPERIMENTAL DETAILS

Hall magnetometers were fabricated from a molecular-beam-epitaxy-grown, δ -doped GaAs/Al_{0.3}Ga_{0.7}As heterostructure, with the two-dimensional electron gas (2DEG) located 75 nm below the wafer surface. The magnetometers were designed as a one-dimensional chain of identical Hall sensors, each having a width of 1.4 μm . The sensor mesas were defined using electron beam lithography and subsequent wet chemical etching in a phosphoric acid solution. Due to underetch and side-wall depletion, the final electrical width of the sensors is 1.2 μm . Ohmic contacts to the 2DEG were realized using an alloyed Ni/AuGe/Ni/Au stack. At temperatures around 4 K, the carrier mobility is 150 000 cm^2/Vs and the sheet electron concentration is $4 \times 10^{11} \text{ cm}^{-2}$, yielding a sensitivity of 0.16 $\mu\text{V}/\mu\text{A G}$. The measurement noise corresponds to 0.05 G.

A superconducting Pb square was defined on the active area of the Hall sensor using e-beam lithography. This step

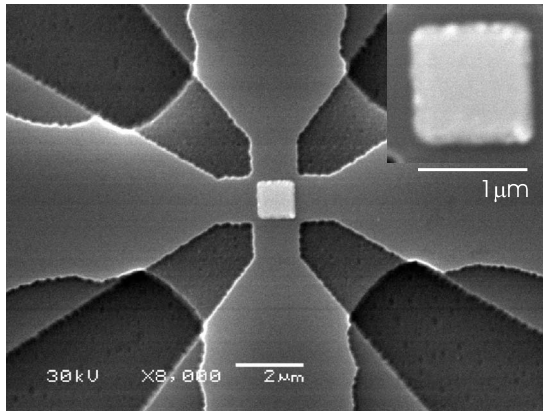


FIG. 1. SEM micrograph of the Hall magnetometer, containing a $1 \times 1 \mu\text{m}^2$ superconducting Pb square. The inset shows a detail of the square.

was aligned relative to the e-beam mesa etch step using alignment markers. The alignment precision is of the order of 50 nm. A Ge/Pb/Ge (5 nm/70 nm/5 nm) multilayer was evaporated onto the substrate in a Varian thermal evaporation chamber. The exact thickness of the Pb layer, measured using x-ray diffraction on a coevaporated reference film, is $t = 72$ nm. From the same film, the coherence length was determined to be $\xi_0 = 37$ nm. After lift-off, the sample was covered with a 100 nm thick Ge layer in order to prevent oxidation of the sides of the Pb square. Contact vias were subsequently etched in the Ge layer with H_2O_2 . The area of the Pb square is $1 \times 1 \mu\text{m}^2$. A scanning electron microscopy (SEM) picture of the finished magnetometer with Pb sample is presented in Fig. 1.

The Hall magnetometry measurements were performed in a commercial physical properties measurement system from Quantum Design. An ac of 150 μA was applied to the Hall magnetometer at a frequency of 2777 Hz. The Hall voltage, which is proportional to the sample magnetization, was recorded using an EG&G Instruments DSP lock-in amplifier. The sample magnetization was measured as a function of applied perpendicular magnetic field, both for increasing and decreasing fields, which was changed in steps of 0.1 mT. Magnetization curves were taken at different temperatures below T_c , ranging from $T = 4.5$ K to $T = 6.5$ K. The final magnetization curves were obtained by subtracting a linear reference curve from the signal of the Hall magnetometer.

III. EXPERIMENTAL RESULTS

Figure 2(a) shows the measured magnetization curve $M(H)$ of the Pb square at $T = 4.5$ K. The applied magnetic field H is also given in terms of flux through the superconducting sample area, expressed in units of ϕ/ϕ_0 , to allow comparison with theory.

The experimental curve displays several typical features. In the increasing $M(H)$ branch, the measured sample magnetization first increases roughly linearly with applied magnetic field, which reflects the Meissner effect in the superconductor. At a certain magnetic field, the magnetization shows

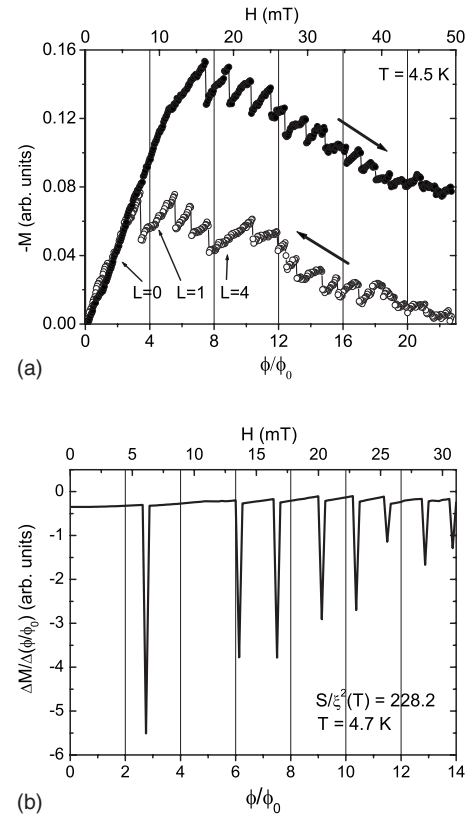


FIG. 2. (a) Experimental magnetization curve at $T = 4.5$ K. The filled and open symbols correspond to increasing and decreasing magnetic fields, respectively. In the decreasing branch vorticities, $L = 0, 1$, and 4 are indicated. (b) Theoretical differential magnetization curve at $T = 4.7$ K based on the full nonlinear Ginzburg-Landau theory (Ref. 13).

a discrete jump, which corresponds to the entrance of a single flux quantum inside the superconductor. Increasing the field further causes more flux quanta to enter the sample, each time is characterized by a jump in the magnetization. This continues until superconductivity is fully suppressed and the sample is in the normal state. In the decreasing $M(H)$ branch, the jumps in the magnetization correspond to flux quanta leaving the sample.

Substantial hysteresis is observed between the increasing and decreasing branches, which is related to the existence of metastable states. Metastability is generally caused by energy barriers between different vortex states. One of these barriers is the Bean-Livingston (BL) surface barrier.¹⁰ It was suggested^{11,14,15} that roughness of the sample boundary, which is usually present in experimental conditions, reduces or even eliminates the BL barrier for flux entry, i.e., in the increasing branch of the magnetization curves. In the decreasing branch, however, the BL barrier remains intact, contributing to metastable states in the superconductor.¹¹ Besides the BL barrier, other energy barriers can exist in our sample, e.g., due to intrinsic flux pinning. It was also shown¹⁵ that vortex penetration can be delayed when the thickness of the sample is larger than the penetration depth, causing the magnetic field inside the sample to be nonuniform. This delay can also contribute to the observed hysteresis.

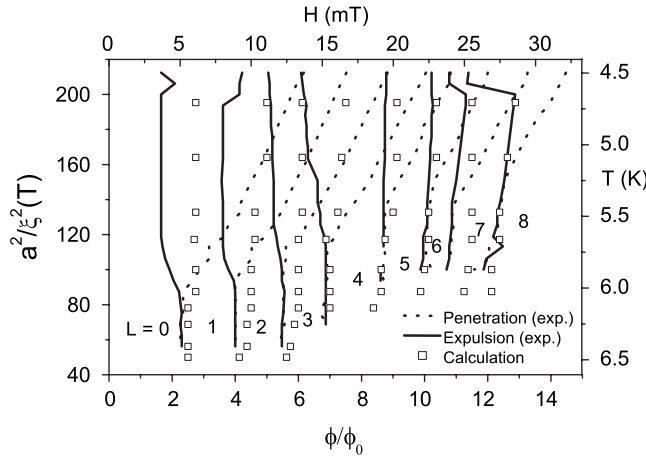


FIG. 3. Phase diagram of the mesoscopic superconducting Pb square. The experimental penetration and expulsion fields as a function of temperature are given by the dashed and solid lines, respectively. The open squares are the calculated results, obtained using the nonlinear GL theory for a thin square.

esis. A consequence of this hysteretic behavior is that the state of the superconducting square for a given field (and temperature) depends on the magnetic history of the sample.

Another feature in the decreasing branch of the magnetization curve in Fig. 2(a) is the fact that certain vorticities are stable in broader field intervals than others. This effect is most pronounced for the states with vorticities $L=1$ and $L=4$.⁹ The enhanced stability is related to the theoretically predicted and experimentally proven commensurability of the symmetry of the vortex pattern with the sample symmetry.

From the magnetization curves measured at different temperatures, a phase diagram was constructed by plotting the vortex penetration and expulsion fields for different vorticities as a function of temperature. This phase diagram is shown in Fig. 3. The dotted and solid lines indicate vortex penetration and expulsion, respectively. Deep in the superconducting state, the effect of hysteresis is clearly seen, characterized by the difference in penetration and expulsion fields for a certain vorticity. The fact that (dotted) penetration lines for certain vorticities cross several (solid) expulsion lines means that the system, at a certain applied magnetic field, can exist in several different metastable states, depending on the path followed in the phase diagram, as discussed before. A large gap is observed between the expulsion lines of $L=5$ and $L=4$, indicating the pronounced stability of the symmetry-matching state $L=4$. A similar gap is observed between the expulsion lines of $L=2$ and $L=1$, indicating the enhanced stability of $L=1$.

At higher temperatures and higher vorticities [i.e., closer to $T_c(H)$], the hysteresis is found to disappear, as indicated by the penetration and expulsion lines in Fig. 3 merging together. In this regime, also the gap between vorticities 5 and 4 is found to be reduced.

IV. COMPARISON WITH THEORETICAL CALCULATIONS

Calculations of the transitions between different vorticities were performed using the nonlinear GL theory for a thin

mesoscopic square and using the method described in Refs. 3, 12, and 13. This procedure consists of a minimization of the GL free energy functional (relative to the normal state) given by

$$G = \int [\Psi^* \hat{L} \Psi + \beta |\Psi|^4 + \alpha |\Psi|^2] d\vec{r}, \quad (1)$$

where $\hat{L} = (-i\hbar \vec{\nabla} - \frac{2e}{c} \vec{A})^2 / 2m^*$, α and β are the GL parameters, and Ψ is the order parameter. This minimization was applied for the superconductor or vacuum boundary conditions,

$$\left(\frac{\hbar \vec{\nabla}}{i} - \frac{2e}{c} \vec{A} \right) \Psi|_n = 0, \quad (2)$$

where \vec{A} is the vector potential and n indicates the normal to the boundary line. Equation (1) assumes that the superconductor is thin; i.e., its thickness t is much smaller than the penetration depth $\lambda(T)$, such that the field in the superconductor coincides with the applied field. It is also assumed that $t \ll \xi(T)$, such that the z dependence of the solution perpendicular to the square cross section can be neglected.

The treatment of the boundary condition [Eq. (2)] is facilitated by applying an analytical gauge transformation,^{1,3,12,13} which reduces it to the Neumann boundary condition $\nabla \Psi|_n = 0$. Furthermore, Ψ is expanded into the eigenfunctions of the linearized GL equation. This allows us to reduce the numerical complexity of the minimization procedure, which was done using a simulated annealing technique. Performing this procedure for different applied fields ϕ/ϕ_0 and $\xi(T)$, the complete phase diagram is obtained.^{3,12,13} It is important to note that by minimizing the GL functional [Eq. (1)], the lowest energy state of the system is obtained, and no metastable states are probed.

Using the area $S = a^2 = 0.9 \mu\text{m}^2$ of the Pb square and $\xi_0 = 37 \text{ nm}$, the results of the calculation can be compared with those of the experimental ones. The smaller effective area of the Pb square with respect to the lithographic area of $1 \times 1 \mu\text{m}^2$ is believed to be due to oxidation of the sample sides, since these were exposed to air during the period between the sample lift-off step and the evaporation of the protective Ge layer. A theoretical differential magnetization curve at $T = 4.7 \text{ K}$, obtained from $M = \frac{1}{2cS} \int_S \vec{r} \times \vec{j}$, is shown in Fig. 2(b). The pronounced peaks indicate the transitions between vortex states with different vorticities. The corresponding transition fields for different temperatures are combined in the phase diagram of Fig. 3 (open squares). Reasonable agreement between experiment and calculation is observed when the phase boundary is approached at relatively high temperatures, where the penetration and expulsion lines meet. An exception is the $L=7$ line, where a deviation between experiment and theory is observed. Also, at lower temperatures, but only for $L > 4$, good agreement is found between the calculation and the expulsion lines. These observations are consistent with the expectation that energy barriers in the sample become weaker close to the phase boundary, i.e., at relatively high temperatures and at lower

temperatures at relatively high fields. In these regions, the used theory adequately describes the system, as is seen in Fig. 3.

In order to explain the deviation of the theory from the experimental phase diagram at low temperatures and low applied magnetic fields, the approximations made in the theory have to be investigated. First of all, the theory assumes the sample to be thin compared to $\xi(T)$ and $\lambda(T)$. Secondly, it also assumes that the length a of the square is much smaller than $\lambda(T)$. Thus, deviations with respect to the experiment can be expected at temperatures well below $T_c(H)$, where both $\xi(T)$ and $\lambda(T)$ significantly decrease. It is also important to keep in mind that the calculations yield the ground state of the system and do not take into account the possibility of metastable states. Therefore, no hysteresis is present in the theoretical results. The occurrence of metastability in our experiment will also contribute to the disagreement with theory at low temperatures, where the order parameter is rather strong. In this regime, substantial energy is required to deform the vortex lattice, resulting in hysteretic behavior, both in the increasing and the decreasing branches of the magnetization curves. At higher temperatures, on the other hand, the order parameter is weak and adapts more easily to the boundary conditions. In this regime, the system can thus be expected to be in the ground state and not to suffer from metastability. In addition, at higher temperatures, the assumptions that $\xi(T)$, $\lambda(T) \gg t$, and $\lambda(T) \gg a$ are better fulfilled. This is nicely seen in Fig. 3, where the penetration and expulsion lines meet toward higher temperatures, and better agreement with theory is obtained.

V. CONCLUSIONS

In conclusion, Hall magnetometry experiments were performed on a mesoscopic superconducting Pb square. The

magnetization curves exhibit discrete jumps, corresponding to the penetration (increasing branch) and expulsion (decreasing branch) of single vortices. From these magnetization curves, an experimental phase diagram was constructed, showing enhanced vortex stabilities for vorticities $L=1$ and $L=4$ in the vortex expulsion deep in the superconducting phase, caused by the commensurability of the vortex pattern symmetry with the sample symmetry. At low temperatures, substantial hysteresis was observed, which was found to be due to metastability in the system, caused by energy barriers between different vortex states. With increasing temperature and/or magnetic field, the hysteretic behavior was found to diminish and eventually disappear. The experimental phase diagram was compared to theoretical calculations using the nonlinear Ginzburg-Landau theory for a thin square. Good agreement between experiment and theory was found relatively close to $T_c(H)$, where no hysteresis was observed in the experiment.

ACKNOWLEDGMENTS

This work was supported by the Belgian Interuniversity Attraction Poles IAP, the Research Fund K.U.Leuven (GOA/2004/02), the Flemish FWO, and the ESF “Nanoscience and Engineering in Superconductivity (NES)” programmes. C.C. acknowledges financial support from Ministerio de Educación y Ciencia (Spain) through FIS2007-63709 and from the Xunta de Galicia (Spain) through the Isidro Parga-Pondal Programme.

-
- ¹L. F. Chibotaru, A. Ceulemans, V. Bruyndoncx, and V. V. Moshchalkov, *Nature* (London) **408**, 833 (2000).
 - ²L. F. Chibotaru, A. Ceulemans, V. Bruyndoncx, and V. V. Moshchalkov, *Phys. Rev. Lett.* **86**, 1323 (2001).
 - ³L. F. Chibotaru, A. Ceulemans, M. Morelle, G. Teniers, C. Carballeira, and V. V. Moshchalkov, *J. Math. Phys.* **46**, 095108 (2005).
 - ⁴V. V. Moshchalkov, X. G. Qiu, and V. Bruyndoncx, *Phys. Rev. B* **55**, 11793 (1997).
 - ⁵V. Bruyndoncx, J. G. Rodrigo, T. Puig, L. Van Look, V. V. Moshchalkov, and R. Jonckheere, *Phys. Rev. B* **60**, 4285 (1999).
 - ⁶A. Kanda, B. J. Baelus, F. M. Peeters, K. Kadowaki, and Y. Ootuka, *Phys. Rev. Lett.* **93**, 257002 (2004).
 - ⁷I. V. Grigorieva, W. Escoffier, J. Richardson, L. Y. Vinnikov, S. Dubonos, and V. Oboznov, *Phys. Rev. Lett.* **96**, 077005 (2006).
 - ⁸A. K. Geim, I. V. Grigorieva, S. V. Dubonos, J. G. S. Lok, J. C. Maan, A. E. Fillippov, and F. M. Peeters, *Nature* (London) **390**, 259 (1997).
 - ⁹M. Morelle, J. Bekaert, and V. V. Moshchalkov, *Phys. Rev. B* **70**, 094503 (2004).
 - ¹⁰C. P. Bean and J. D. Livingston, *Phys. Rev. Lett.* **12**, 14 (1964).
 - ¹¹P. S. Deo, V. A. Schweigert, and F. M. Peeters, *Phys. Rev. B* **59**, 6039 (1999).
 - ¹²L. F. Chibotaru, G. Teniers, A. Ceulemans, and V. V. Moshchalkov, *Phys. Rev. B* **70**, 094505 (2004).
 - ¹³C. Carballeira, G. Teniers, L. F. Chibotaru, A. Ceulemans, M. Morelle, and V. V. Moshchalkov, *Europhys. Lett.* **75**, 936 (2006).
 - ¹⁴A. K. Geim, S. V. Dubonos, I. V. Grigorieva, K. S. Novoselov, F. M. Peeters, and V. A. Schweigert, *Nature* (London) **407**, 55 (2000).
 - ¹⁵P. S. Deo, V. A. Schweigert, F. M. Peeters, and A. K. Geim, *Phys. Rev. Lett.* **79**, 4653 (1997).